

Electron-Transfer Protein Reactivities. Kinetic Studies of the Oxidation of Horse Heart Cytochrome *c*, *Chromatium vinosum* High Potential Iron-Sulfur Protein, *Pseudomonas aeruginosa* Azurin, Bean Plastocyanin, and *Rhus vernicifera* Stellacyanin by Pentaamminepyridineruthenium(III)

Diane Cummins and Harry B. Gray*¹

Contribution No. 5470 from the Arthur Amos Noyes Laboratory of Chemical Physics, California Institute of Technology, Pasadena, California 91125.
Received November 29, 1976

Abstract: Kinetic studies of the oxidation of ferrocycytochrome *c*, HiPIP, azurin, plastocyanin, and stellacyanin by $[\text{Ru}(\text{NH}_3)_5\text{py}]^{3+}$ have been performed, giving: second-order rate constants of 1.86×10^4 (25 °C, pH 5.3, $\mu = 0.5$ M), 1.10×10^3 (25 °C, pH 6.5, $\mu = 0.5$ M), 2.00×10^3 (25 °C, pH 6.5, $\mu = 0.1$ M), 7.10×10^3 (25 °C, pH 6.5, $\mu = 0.5$ M), and 1.95×10^5 (25 °C, pH 6.5, $\mu = 0.1$ M) $\text{M}^{-1} \text{s}^{-1}$; ΔH^\ddagger of 8.4, 9.4, 8.8, 5.6, and 6.7 kcal/mol; and ΔS^\ddagger of -11, -13, -14, -22, and -12 eu, respectively. The rate of oxidation of the outer-sphere reductant $[\text{Co}(\text{terpy})_2]^{2+}$ has also been studied, giving the second-order rate constant $1.61 \times 10^3 \text{ M}^{-1} \text{ s}^{-1}$, $\Delta H^\ddagger = 6.2$ kcal/mol, and $\Delta S^\ddagger = -23$ eu. The electron-transfer rate parameters have been analyzed in terms of relative Marcus theory to give electrostatics-corrected protein self-exchange rate constants (k_{11}^{corr}). Comparison of the k_{11}^{corr} values with those from analogous redox reactions with $\text{Ru}(\text{NH}_3)_6^{2+}$, $[\text{Co}(\text{phen})_3]^{3+}$, and $[\text{Fe}(\text{EDTA})]^{2-}$ indicates that $[\text{Ru}(\text{NH}_3)_5\text{py}]^{3+}$ facilitates electron transfer from metalloproteins. This enhancement of reactivity is attributed to penetration of the protruding edge of the π -conjugated pyridine ligand into the protein interior, which allows direct protein-reagent redox center orbital overlap in the transition state for electron transfer. The ionic strength dependence data for each protein oxidation reaction are fitted to Marcus theory and transition-state theory equations describing such dependences, and the charges on the proteins are thus extracted. The results of one such study suggest that phosphate ions bind to ferrocycytochrome *c*, thereby reducing the effective charge on the protein.

Studies of the electron-transfer reactions between metalloproteins and inorganic reagents are continuing in our laboratory. Recent evidence has suggested that electron transfer between horse heart cytochrome *c* and certain inorganic redox reagents takes place by an outer-sphere mechanism involving the partially exposed heme edge,²⁻⁴ and it has been proposed that the degree of access of any given substrate to this edge depends on its size, charge, and surface properties.⁵

In addition to cytochrome *c*, electron-transfer mechanistic studies in our laboratory have centered on the blue copper proteins *Rhus vernicifera* stellacyanin, bean plastocyanin, and *Pseudomonas aeruginosa* azurin, as well as on *Chromatium vinosum* high potential iron-sulfur protein (HiPIP). Structural considerations suggest that outer-sphere electron transfer is favored in the case of HiPIP, and, in fact, several studies have shown that the protein employs such a mechanism.⁶⁻⁹ The cubelike $\text{Fe}_4\text{S}_4\text{S}_4^*$ cluster is completely buried, the closest distance between it and the protein surface being 4.5 Å.¹⁰

X-ray crystal structures are not yet available for any of the blue copper proteins, but a detailed structural model of the blue copper site has emerged as a result of various spectroscopic studies.¹¹ Specifically, the site in bean plastocyanin is proposed to be flattened tetrahedral, the four coordinated ligands being two histidines (His-38 and -88), Cys-85, and a backbone peptide nitrogen or oxygen.¹² The other blue proteins are expected to possess similar coordination environments. If this coordination geometry is correct, then outer-sphere electron transfer in these proteins is expected to be facile. Kinetic studies with various reagents have verified this expectation.¹³⁻¹⁵ It is believed from magnetic resonance and fluorescence measurements that certain of the blue copper sites are substantially buried in solvent-inaccessible protein interiors, and kinetic studies are consistent with this belief.¹¹

In previous papers,^{5,11} a model has been presented for interpreting the kinetics of protein electron-transfer reactions within the framework of Marcus outer-sphere theory. In this

model, the contributions to the activation free energy from the reagent reactivity, general electrostatic influences, and the thermodynamic driving force for the overall reaction are factored out to leave a quantity which is characteristic of the protein and the particular mechanism of electron transfer which it undergoes with the reagent. This quantity is the electrostatics-corrected self-exchange rate constant for the protein, k_{11}^{corr} . The application of this analysis to the available data on protein redox reactions has led to the definition of a "kinetic accessibility" scale, and an analysis of the factors controlling protein-small molecule and protein-protein reactivities. The data reported in this paper allow extension of this analysis, over a range of proteins, to the reagent $[\text{Ru}(\text{NH}_3)_5\text{py}]^{3+}$, and comparison of the results with those of the two reagents $[\text{Fe}(\text{EDTA})]^{2-}$ and $[\text{Co}(\text{phen})_3]^{3+}$.

Experimental Section

Reagent grade chemicals and distilled water were used throughout. Nitrogen gas passed through two chromous scrubbing towers, to remove oxidizing impurities, was used to deoxygenate kinetic solutions, and argon gas, purified in an identical manner, was used in the preparation of pentaamminepyridineruthenium(II).

Horse heart cytochrome *c* (type VI) was obtained from Sigma Chemical Co. *Rhus vernicifera* stellacyanin and bean plastocyanin were isolated and purified, as described previously,¹³ to ratios A_{280}/A_{604} of 5.60 and A_{278}/A_{597} of 1.17, respectively. Azurin from *Pseudomonas aeruginosa* was purified by the method of Ambler and Wynn¹⁶ to a ratio A_{628}/A_{280} of 0.58, and was stored refrigerated, after Millipore filtering, in sterile vials in 0.05 M, pH 5.1, ammonium acetate buffer. HiPIP extracted from cells of *Chromatium vinosum* was purified to a ratio A_{283}/A_{388} of 2.52, Millipore filtered into sterile vials, and stored refrigerated in 0.02 M Tris (pH 8.0)-0.4 M NaCl.

$[\text{Ru}(\text{NH}_3)_5\text{py}]\text{ClO}_4$ was prepared by modifying the literature procedure.¹⁷ Hexaammineruthenium(III) trichloride (Matthey Bishop, Inc.) was converted to chloropentaammineruthenium(III) dichloride as described. Silver(I) oxide (0.158 g) was suspended in water (ca. 4 mL), warmed, and stirred, and sufficient trifluoroacetic

acid was added dropwise to dissolve it. Chloropentaammineruthenium(III) dichloride (0.200 g) was digested with this solution until the precipitation of silver(I) chloride was complete. After filtering, the resultant solution of aquopentaammineruthenium(III) trifluoroacetate was deoxygenated by bubbling with argon (ca. 15 min) and reduced with zinc amalgam, and then the pH was raised to about 5 by dropwise addition of sodium hydroxide (2 M) to give a yellow solution. A five- to sixfold excess of pyridine was added, and the argon bubbling was continued during the approximately 30-min reaction time. The bright orange reaction mixture was filtered, and solid sodium perchlorate was added very slowly, while the solution was bubbled with argon, until precipitation of the bright yellow $[\text{Ru}(\text{NH}_3)_5\text{py}](\text{ClO}_4)_2$ was complete. (Sealing the flask and refrigeration for 1 h at this stage helped increase the product yield.) The product was filtered, washed with ether, and dried carefully in a vacuum desiccator. The ruthenium(II) species could be recrystallized from warm water with some loss in yield.¹⁸

$[\text{Ru}(\text{NH}_3)_5\text{py}](\text{ClO}_4)_2$ was dissolved in a minimum of acetone and ceric perchlorate solution (0.025 M in 3.0 M perchloric acid, G. Frederick Smith Chemical Co.) was added dropwise, and with stirring, until the color change from orange to pale yellow was complete. Removal of the acetone, by rotary evaporation at 20 °C, resulted in the formation of the pale yellow $[\text{Ru}(\text{NH}_3)_5\text{py}](\text{ClO}_4)_3$. The product was recrystallized from warm perchloric acid (0.1 M), filtered, washed with ether, dried, and stored in a vacuum desiccator. Anal. Calcd: C, 10.66; H, 3.58; N, 14.91; Cl, 18.87. Found: C, 10.62; H, 3.64; N, 14.69; Cl, 17.36.¹⁹

$[\text{Co}(\text{terpy})_2]\text{Cl}_2$ was prepared by a minor modification of the procedure used by Baker et al.²⁰ to obtain the corresponding ClO_4^- salt.

Solutions of ferrocyanochrome *c* were prepared by dissolving the oxidized protein in 2 to 3 mL of the appropriate buffer and reducing with a 20-fold excess of $\text{Fe}(\text{HEDTA})^-$. Excess $\text{Fe}(\text{HEDTA})^-$ and $\text{Fe}(\text{HEDTA})$ were removed using a Sephadex G-25 gel filtration column (2 × 15 cm, Sigma Chemical Co.) equilibrated with the appropriate deoxygenated buffer. The reduced protein was loaded onto the column, eluted with deoxygenated buffer, and diluted to the desired volume. Solutions of the proteins stellacyanin, azurin, plastocyanin, and HiPIP were first obtained in the appropriate buffer by dialyzing small volumes of concentrated oxidized protein (usually 2 to 10 mL) against at least three changes (500 mL) of that buffer. Stellacyanin and HiPIP were prepared in reduced form by diluting accurately to a known volume and concentration, deoxygenating in a serum-capped bottle by gently bubbling with nitrogen, and reducing with a molar equivalent of ascorbic acid. No attempt was made to remove the dehydroascorbate product. Solutions of reduced azurin and plastocyanin were prepared by diluting to the desired volume (usually ca. 50 mL) and reducing with a 20-fold excess of $\text{Fe}(\text{HEDTA})^-$. The protein solutions were then freed of excess reductant by dialyzing, under a constant stream of argon, in a hollow fiber Dow beaker dialyzer (Bio-Rad Laboratories) against about 2 L of argon-saturated buffer.

Nitrogen was carefully bubbled through all solutions for 20 min prior to kinetic measurements. Most solutions were stored in serum-capped round-bottomed flasks, each with a nitrogen inlet tube and a glass luerlock fitting. They were then transferred to the stopped-flow apparatus through Teflon tubing connected to the inlet port. The use of an all-glass system was particularly important for transferring solutions of $[\text{Ru}(\text{NH}_3)_5\text{py}]^{3+}$, as they were reduced during passage through stainless steel needles.

Observations of the stability of $[\text{Ru}(\text{NH}_3)_5\text{py}]^{3+}$ in various media²¹ dictated the use of a limited range of buffer solutions: acetate and phosphate buffers, with sodium sulfate added to give the desired ionic strength, were found to be suitable and gave solutions of $[\text{Ru}(\text{NH}_3)_5\text{py}]^{3+}$ which could be stored for the duration of an experiment without observable decomposition.

Kinetic Measurements. Kinetic measurements were performed on a Durrum Model D-110 stopped-flow spectrophotometer. Solutions to be mixed were allowed to temperature equilibrate at least 15 min at room temperature and 30 min at other temperatures. Data collection was carried out as described previously.¹³ The rates of oxidation were measured at the following wavelengths: ferrocyanochrome *c*, 550 nm ($\Delta\epsilon = 18.5 \times 10^3 \text{ M}^{-1} \text{ cm}^{-1}$)²²; stellacyanin, 604 nm ($\Delta\epsilon = 4.1 \times 10^3 \text{ M}^{-1} \text{ cm}^{-1}$)²³; azurin, 625 nm ($\Delta\epsilon = 5.7 \times 10^3 \text{ M}^{-1} \text{ cm}^{-1}$)²⁴; plastocyanin, 597 nm ($\Delta\epsilon = 4.5 \times 10^3 \text{ M}^{-1} \text{ cm}^{-1}$)²⁵; HiPIP, 500 nm ($\Delta\epsilon = 6.3 \times 10^3 \text{ M}^{-1} \text{ cm}^{-1}$)²⁶; $[\text{Co}(\text{terpy})_2]^{2+}$, 408 nm ($\Delta\epsilon$

($[\text{Ru}(\text{NH}_3)_5\text{py}]^{3+}$ reduction) = $7.76 \times 10^3 \text{ M}^{-1} \text{ cm}^{-1}$).¹⁷ An absorbance change of 0.1 was monitored in all cases except stellacyanin, where a change of 0.05 was used. The oxidant concentration was always in pseudo-first-order excess over the reductant and was varied over as wide a range as was possible in each experiment. In the cases where the oxidation was carried out against the driving force for the reaction, that is, where $E^0_{\text{oxidant}} - E^0_{\text{reductant}} < 0$, care was taken to ensure that lowest oxidant concentrations were high enough to give 90% completion of the reaction: $\text{Ru}^{3+} + \text{reduced protein} \rightleftharpoons \text{Ru}^{2+} + \text{oxidized protein}$. That is, at equilibrium, $[\text{oxidized protein}]/[\text{reduced protein}] \geq 9$. Data points were then collected for the reaction to this equilibrium, and all other parameters for analysis of the data were measured independently.

Data Analysis. Plots of $\log(A_t - A_\infty)$ vs. t were made to verify first-order kinetic behavior; for each reaction the pseudo-first order rate constant (k_{obsd}) was obtained from the slope of the line determined by a linear least-squares method.

The data obtained for the two lowest oxidant concentrations for the oxidation of azurin were also analyzed as "approach-to-equilibrium",²⁷ and the rate constants so obtained were compared with those obtained from the $\log(A_t - A_\infty)$ vs. t plots.

The concentration and temperature dependences of each reaction were analyzed using weighted least squares. The weighting factors for the concentration dependence fits were the square of the inverse of the standard deviation from the mean of the multiple determinations (from four to eight) done from one filling of the drive syringes. For the temperature dependence data, the standard deviations in k_{obsd} , determined as above, were used to propagate the standard deviations in $\ln(k_{\text{obsd}}/T)$. The weighting factors for the Eyring plots were then the square of the inverse of standard deviations in $\ln(k_{\text{obsd}}/T)$.

The ionic strength dependences of the rate constants for each protein oxidation reaction were analyzed according to various theories (see Results), using nonweighted least squares.

Reduction Potential Measurements. Standard electrochemical techniques were used to measure the reduction potentials of $[\text{Co}(\text{phen})_3]^{3+}$, $[\text{Co}(\text{terpy})_2]^{3+}$, $[\text{Co}(\text{bipy})_3]^{3+}$, and $[\text{Ru}(\text{NH}_3)_5\text{py}]^{3+}$. As the potentials were to be used in the reaction rate data analysis, the measurements were carried out in buffers corresponding to those used in kinetic measurements. The electrode used was a platinum ball attached to a fine platinum wire sealed in glass. Potentials were measured with respect to a calomel electrode saturated with sodium chloride.

Cyclic voltammograms of the complexes $[\text{Co}(\text{phen})_3]^{3+}$, $[\text{Co}(\text{terpy})_2]^{2+}$, $[\text{Co}(\text{bipy})_3]^{2+}$, and $[\text{Ru}(\text{NH}_3)_5\text{py}]^{3+}$ were obtained on an X-Y recorder at sweep rates of 120 to 160 mV/s. The potentials at the anodic and cathodic peaks were then measured accurately by sweeping the potential manually, and were used to calculate the reduction potential ($E_{1/2}$) of the complex [$E_{1/2} = (E_{\text{PA}} + E_{\text{PC}})/2$, where E_{PA} = anodic peak potential and E_{PC} = cathodic peak potential, and this differs from the formal electrode potential, E^0 , by $30 \log(D_{\text{III}}/D_{\text{II}})$ mV, where D_{III} and D_{II} are the diffusion coefficients of the metal(III) and metal(II) complexes, respectively].

Differential pulsed polarograms were also recorded, in a similar manner, for $[\text{Ru}(\text{NH}_3)_5\text{py}]^{3+}$, both as a second potential measurement, and as a check for material purity.

Results

Kinetic Measurements. First-order plots of absorbance-time data for the oxidation of ferrocyanochrome *c*, stellacyanin(I), and the outer-sphere reductant $[\text{Co}(\text{terpy})_2]^{2+}$ were found to be linear for greater than three reaction half-lives. The analogous plots for the oxidation of azurin(I) were similarly linear for the high oxidant concentrations, but for the two lowest concentrations of the oxidant (ca. 88% and ca. 93% completion of reaction) they were linear for only 2 and 2.2 half-lives, respectively. The linear portions of these plots were used to obtain pseudo-first-order rate constants, and these values were found to be, at most, 10% higher than those obtained using the function for reaction to equilibrium.²⁸ The reasonable agreement observed between these two analyses suggested that the use of the simple first-order treatment was justified in these cases, and that the error in k_{obsd} so obtained was in line with experimental error.

The simple first-order plots for the oxidation of HiPIP and

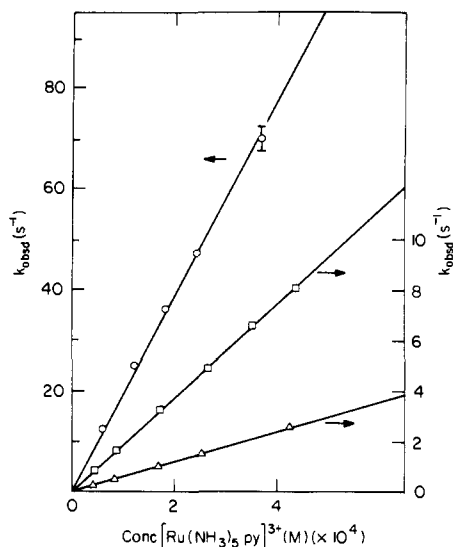


Figure 1. The dependences of the observed rate constants on the concentration of $[\text{Ru}(\text{NH}_3)_5\text{py}]^{3+}$ at 25 °C: (O) stellacyanin (pH 6.5 phosphate, $\mu = 0.1$ M); (□) ferrocyanochrome *c* (pH 5.3 acetate, $\mu = 0.5$ M); (Δ) ferrocyanochrome *c* (pH 5.0 acetate, $\mu = 0.1$ M).

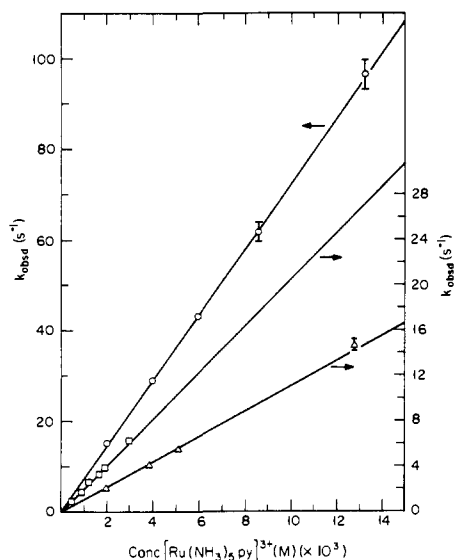


Figure 2. The dependences of the observed rate constants on the concentration of $[\text{Ru}(\text{NH}_3)_5\text{py}]^{3+}$ at 25 °C: (O) plastocyanin (pH 6.5 phosphate, $\mu = 0.5$ M); (□) azurin (pH 6.5 phosphate, $\mu = 0.1$ M); (Δ) HiPIP (pH 6.5 phosphate, $\mu = 0.5$ M).

plastocyanin(I) were again linear for three reaction half-lives, for all but the lowest concentration of $[\text{Ru}(\text{NH}_3)_5\text{py}]^{3+}$ (90% completion), where they were linear for about 80% of the reaction. The rate constants (k_{obsd}) from these latter were used, as justified for the azurin(I) oxidation.

The dependence of observed rate constants on $[\text{Ru}(\text{NH}_3)_5\text{py}]^{3+}$ concentration is shown in Figures 1–3, and on temperature is illustrated in Figure 4. In all cases, the rate law is first order in each reactant over the range of oxidant concentrations accessible. Second-order rate constants and activation parameters are summarized in Table I.

Data describing the dependence of each protein oxidation rate on ionic strength are collected in Table II. The rate of oxidation of ferrocyanochrome *c* is observed to increase with ionic strength in both acetate and phosphate media (Figure 5). The dependence in the latter, however, is somewhat less than might be expected from the approximately unit change in pH alone. The rates of oxidation of stellacyanin(I), azurin(I), HiPIP, and plastocyanin(I) each decrease with increasing

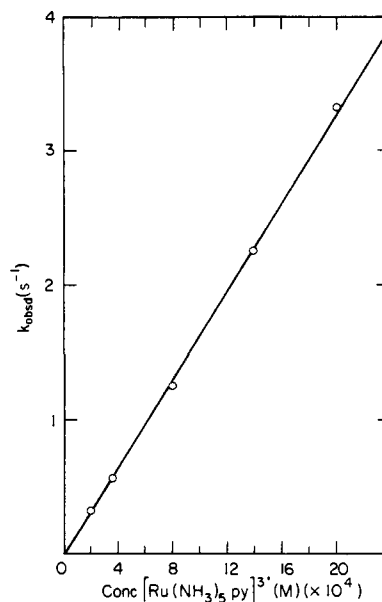


Figure 3. The dependence of the observed rate constants for $[\text{Co}(\text{terpy})_2]^{2+}$ oxidation on the concentration of $[\text{Ru}(\text{NH}_3)_5\text{py}]^{3+}$ at 25 °C, pH 6.5 phosphate, $\mu = 0.1$ M.

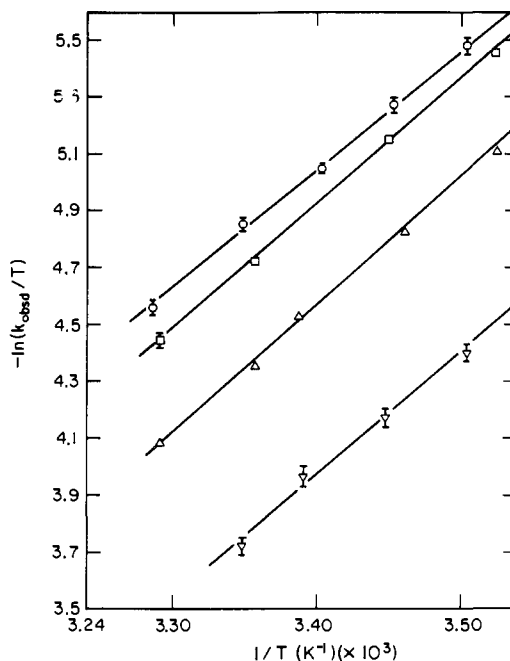


Figure 4. Eyring plots of the rate data for oxidation by $[\text{Ru}(\text{NH}_3)_5\text{py}]^{3+}$: (O) ferrocyanochrome *c* (pH 5.3 acetate, $\mu = 0.5$ M, $[\text{Ru}(\text{NH}_3)_5\text{py}]^{3+} = 1.285 \times 10^{-4}$ M); (▽) ferrocyanochrome *c* (pH 5.3 acetate, $\mu = 0.5$ M, $[\text{Ru}(\text{NH}_3)_5\text{py}]^{3+} = 3.718 \times 10^{-4}$ M); (□) azurin (pH 6.5 phosphate, $\mu = 0.1$ M, $[\text{Ru}(\text{NH}_3)_5\text{py}]^{3+} = 1.23 \times 10^{-3}$ M); (Δ) azurin (pH 6.5 phosphate, $\mu = 0.1$ M, $[\text{Ru}(\text{NH}_3)_5\text{py}]^{3+} = 1.905 \times 10^{-3}$ M).

ionic strength. The dependences for azurin(I) and plastocyanin(I) are shown in Figure 6. The lines are the least-squares fits to three functions which have been used to describe ionic strength dependences.^{5,11} Briefly, the transition-state theory equation is:

$$\ln k = \ln k_0 + \frac{(2Z_1Z_2 + Z_2^2)\alpha\sqrt{\mu}}{1 + \kappa R_1} - \frac{Z_2^2\alpha\sqrt{\mu}}{1 + \kappa R_2} \quad (1)$$

which is often simplified to

$$\ln k = \ln k_0 + 2Z_1Z_2\alpha\sqrt{\mu} \quad (2)$$

Table I. Rate Constants at 25 °C and Activation Parameters for Oxidations by $[\text{Ru}(\text{NH}_3)_5\text{py}](\text{ClO}_4)_3$

Reductant	$k_{12}, \text{M}^{-1} \text{s}^{-1} (\sigma)^a$	$\Delta H^\ddagger, \text{kcal/mol}^b$	$\Delta S^\ddagger, \text{eu}^c$
$[\text{Co}(\text{terpy})_2]^{2+ d}$	1.61×10^3	6.2	-23
Ferrocyanochrome c^e	1.86×10^4	8.4	-11
Ferrocyanochrome c^f	5.96×10^3	8.0	-14
Stellacyanin g	$1.94 (0.05) \times 10^5$	6.7	-12
Azurin h	2.00×10^3	8.8	-14
HiPIP i	$1.10 (0.03) \times 10^3$	9.4	-13
Plastocyanin j	$7.10 (0.14) \times 10^3$	5.6	-22

^a The standard deviation of the slope as given by the weighted least-squares analysis, included as an indication of goodness of fit; where σ is not given, it is significantly smaller than 0.01. ^b Average ΔH^\ddagger from the two independent determinations quoted to two figures. ^c Average ΔS^\ddagger from the two independent determinations quoted to two figures. ^d pH 6.5, phosphate ($\mu = 0.05 \text{ M}$), total $\mu = 0.1 \text{ M}$ (Na_2SO_4), $[\text{Co}(\text{terpy})_2]^{2+} = 1.3 \times 10^{-5} \text{ M}$, $[\text{Ru}(\text{NH}_3)_5\text{py}]^{3+} = 2 \times 10^{-4}$ to $2 \times 10^{-3} \text{ M}$. ^e pH 5.3, acetate ($\mu = 0.5 \text{ M}$), [ferrocyanochrome c] = $3 \times 10^{-6} \text{ M}$, $[\text{Ru}(\text{NH}_3)_5\text{py}]^{3+} = 4.4 \times 10^{-5}$ to $4.4 \times 10^{-4} \text{ M}$. ^f pH 5.0, acetate ($\mu = 0.1 \text{ M}$), [ferrocyanochrome c] = $3 \times 10^{-6} \text{ M}$, $[\text{Ru}(\text{NH}_3)_5\text{py}]^{3+} = 4.26 \times 10^{-5}$ to $4.26 \times 10^{-4} \text{ M}$. ^g pH 6.5, phosphate ($\mu = 0.05 \text{ M}$), total $\mu = 0.1 \text{ M}$ (Na_2SO_4), [stellacyanin] = $6 \times 10^{-6} \text{ M}$, $[\text{Ru}(\text{NH}_3)_5\text{py}]^{3+} = 6.13 \times 10^{-5}$ to $3.68 \times 10^{-4} \text{ M}$. ^h pH 6.5, phosphate ($\mu = 0.05 \text{ M}$), total $\mu = 0.1 \text{ M}$ (Na_2SO_4), [azurin] = $9 \times 10^{-6} \text{ M}$, $[\text{Ru}(\text{NH}_3)_5\text{py}]^{3+} = 4.2 \times 10^{-4}$ to $2.94 \times 10^{-3} \text{ M}$. ⁱ pH 6.5, phosphate ($\mu = 0.25 \text{ M}$), total $\mu = 0.5 \text{ M}$ (Na_2SO_4), [HiPIP] = $8.5 \times 10^{-6} \text{ M}$, $[\text{Ru}(\text{NH}_3)_5\text{py}]^{3+} = 1.92 \times 10^{-3}$ to $1.28 \times 10^{-2} \text{ M}$. ^j pH 6.5, phosphate ($\mu = 0.25 \text{ M}$), total $\mu = 0.5 \text{ M}$ (Na_2SO_4), [plastocyanin] = $1.11 \times 10^{-5} \text{ M}$, $[\text{Ru}(\text{NH}_3)_5\text{py}]^{3+} = 1.98 \times 10^{-3}$ to $1.32 \times 10^{-2} \text{ M}$.

but this simplification is only valid when all radii are equal and the ionic strength is low enough that $1 \gg \kappa R$. The third equation is that derived from Marcus theory:

$$\ln k = \ln k_0 - 3.576 \left[\frac{\exp(-\kappa R_1)}{1 + \kappa R_2} + \frac{\exp(-\kappa R_2)}{1 + \kappa R_1} \right] \times \left[\frac{Z_1 Z_2}{R_1 + R_2} \right] \quad (3)$$

Data required in the calculations are collected in Table III, and the parameters for the fits for each protein to these equations are given in Table IV.

Reduction Potentials. The cyclic voltammograms for $[\text{Co}(\text{phen})_3]^{3+}$ in phosphate buffer (pH 6.5, $\mu = 0.1 \text{ M}$), $[\text{Co}(\text{bipy})_3]^{2+}$ and $[\text{Ru}(\text{NH}_3)_5\text{py}]^{3+}$ in phosphate (pH 6.5, $\mu = 0.05 \text{ M}$)/ Na_2SO_4 ($\mu = 0.05 \text{ M}$) buffer, and $[\text{Co}(\text{terpy})_2]^{2+}$ in each of these media display highly reversible behavior at sweep rates 120 to 160 mV/s, with no evidence for chemical reactions preceding or subsequent to the electrode reactions. The differential pulsed polarogram of $[\text{Ru}(\text{NH}_3)_5\text{py}]^{3+}$ in phosphate (pH 6.5, $\mu = 0.1 \text{ M}$) shows a single symmetrical peak, with no trace of any electrochemically active impurities, such as $[\text{Ru}(\text{NH}_3)_5\text{H}_2\text{O}]^{3+}$. The potential obtained by this technique agrees well with that measured by cyclic voltammetry. The values for the reduction potentials are collected in Table III. Standard values obtained²⁹ previously for the inorganic reagents are included for comparison.

The cyclic voltammograms of the four complexes in phosphate (pH 6.0, $\mu = 0.05 \text{ M}$)/ Na_2SO_4 ($\mu = 0.45 \text{ M}$), phosphate (pH 6.7, $\mu = 0.05 \text{ M}$)/ NaCl ($\mu = 0.45 \text{ M}$), and phosphate (pH 6.9, $\mu = 0.05 \text{ M}$)/ NaCl ($\mu = 0.05 \text{ M}$) were highly complex. In most cases, the major anodic and cathodic peaks corresponded to those observed in the "clean" systems described above, but, in all cases, one or more additional peaks were observed in both the anodic and cathodic half-cycles. Thus, at high ionic strengths, or, in the presence of chloride ions, reduction potentials could not be obtained, probably because of chemical reactions preceding reaction at the electrode.³⁰⁻³²

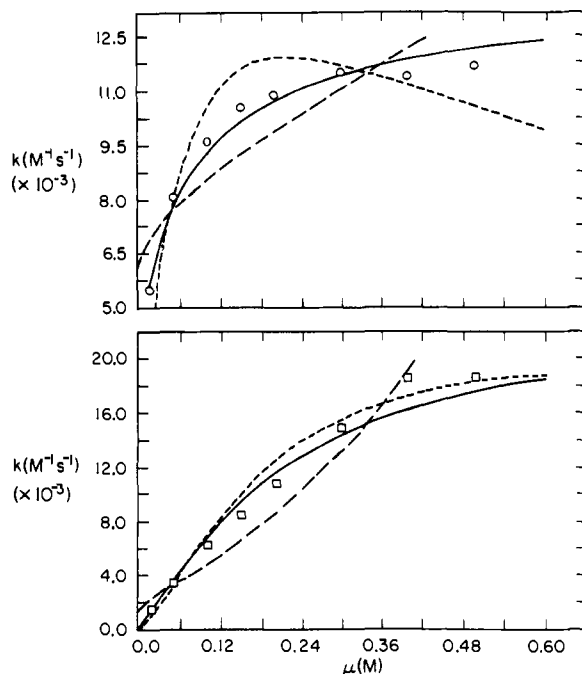


Figure 5. The dependence of the second-order rate constants on ionic strength for the oxidation of ferrocyanochrome c by $[\text{Ru}(\text{NH}_3)_5\text{py}]^{3+}$: (O) experimental data, 25 °C, pH 6.5 phosphate; (□) experimental data, 25 °C, pH 5.3 acetate; theoretical fits: (—) Marcus eq 3; (---) eq 2; (- - -) transition-state eq 1.

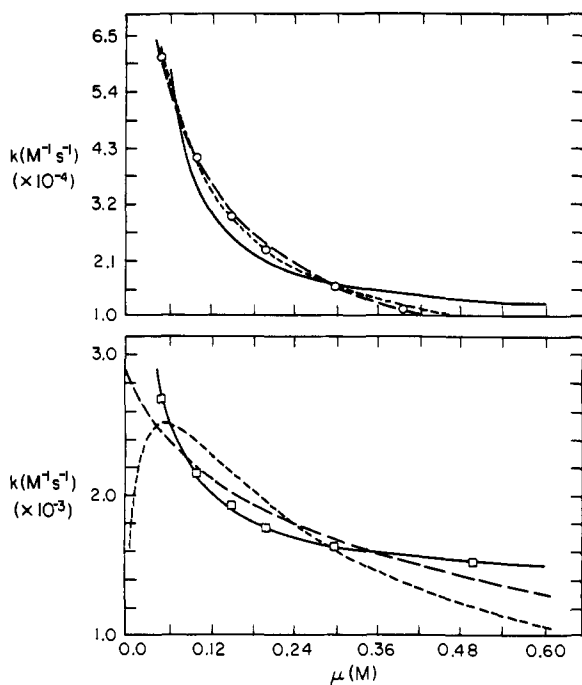


Figure 6. The dependence of the second-order rate constants on ionic strength for oxidation by $[\text{Ru}(\text{NH}_3)_5\text{py}]^{3+}$. 25 °C, pH 6.5 phosphate. Experimental data: (O) plastocyanin; (□) azurin; Theoretical fits: (—) Marcus eq 3; (---) eq 2; (- - -) transition-state eq 1.

Discussion

Inspection of the rate parameters for the oxidation of the reduced proteins and $[\text{Co}(\text{terpy})_2]^{2+}$ by $[\text{Ru}(\text{NH}_3)_5\text{py}]^{3+}$ suggests that, in each case, the electron transfer takes place by a simple outer-sphere mechanism. Both in these and related studies³³ involving $\text{Ru}(\text{NH}_3)_5\text{L}^{3+}$ oxidants, where L is a pyridine derivative, we have found no evidence that would require us to postulate the intermediacy of an L radical anion during

Table II. Ionic Strength Dependences of Rate Data for [Ru(NH₃)₅py](ClO₄)₃ Oxidations

Protein	μ , M ^a	k_{obsd} , s ⁻¹ (σ) ^b	[[Ru(NH ₃) ₅ py] ³⁺], M ($\times 10^4$)	k , M ⁻¹ s ⁻¹ ($\times 10^{-3}$)	k_{av} , ^c M ⁻¹ s ⁻¹ ($\times 10^{-3}$)
Ferrocyanochrome <i>c</i> ^d	0.02	0.129 (0.004)	0.858	1.50	1.50
		0.202 (0.009)	1.358	1.49	
	0.05	0.311 (0.010)	0.901	3.45	3.41
		0.465 (0.011)	1.382	3.37	
	0.10	0.515 (0.004)	0.841	6.13	6.15
		0.916 (0.021)	1.488	6.16	
	0.15	0.747 (0.050)	0.877	8.52	8.49
		1.233 (0.027)	1.457	8.46	
	0.20	0.897 (0.047)	0.862	10.41	10.66
		1.567 (0.042)	1.440	10.90	
Ferrocyanochrome <i>c</i> ^e	0.02	0.994 (0.021)	1.833	5.42	5.48
		0.685 (0.014)	1.238	5.53	
	0.05	1.67 (0.030)	2.100	7.95	8.03
		0.845 (0.013)	1.043	8.10	
	0.10	1.77 (0.06)	1.839	9.60	9.61
		1.15 (0.02)	1.191	9.62	
	0.15	1.90 (0.03)	1.818	10.45	10.54
		1.38 (0.03)	1.302	10.62	
	0.20	1.98 (0.01)	1.817	10.91	10.89
		1.32 (0.02)	1.213	10.87	
Stellacyanin ^f	0.05	1.99 (0.03)	1.739	11.44	11.49
		1.37 (0.02)	1.186	11.54	
	0.40	2.24 (0.02)	2.015	11.11	11.37
		1.54 (0.02)	1.328	11.62	
	0.50	2.15 (0.03)	1.867	11.52	11.67
		1.33 (0.02)	1.127	11.81	
	0.92	26.2 (0.7)	1.027	255.1	254.5
		48.9 (1.7)	1.926	253.9	
	0.05	35.2 (1.3)	1.285	256.8	246.3
		44.1 (1.9)	1.870	235.8	
Azurin ^f	0.10	21.7 (0.4)	1.042	208.3	210.9
		41.7 (2.1)	1.953	213.5	
	0.15	18.6 (0.8)	1.043	178.3	181.2
		36.0 (0.9)	1.955	184.1	
	0.2	18.0 (1.2)	1.060	169.8	168.2
		33.1 (0.7)	1.988	166.6	
	0.3	14.7 (0.7)	1.080	136.1	141.4
		29.7 (1.5)	2.025	146.7	
	0.4	13.4 (0.3)	1.085	123.5	124.7
		25.6 (1.1)	2.035	125.8	
HiPIP ^f	0.5	12.6 (0.4)	1.105	114.0	113.5
		23.4 (0.5)	2.072	112.9	
	0.05	1.24 (0.02)	4.698	2.64	2.69
		2.41 (0.04)	8.809	2.74	
	0.10	1.08 (0.03)	4.858	2.22	2.17
		1.94 (0.06)	9.110	2.13	
	0.15	0.96 (0.05)	4.787	2.01	1.92
		1.66 (0.07)	8.976	1.85	
	0.20	0.87 (0.05)	4.747	1.83	1.78
		1.53 (0.02)	8.900	1.72	
Plastocyanin ^f	0.30	0.81 (0.01)	4.740	1.71	1.63
		1.38 (0.04)	8.888	1.55	
	0.50	0.75 (0.01)	4.795	1.56	1.52
		1.30 (0.05)	8.990	1.44	
	0.05	7.20 (0.34)	17.05	4.223	
	0.10	4.23 (0.03)	17.13	2.469	
	0.15	3.37 (0.14)	17.15	1.965	
	0.20	3.10 (0.11)	17.15	1.808	
	0.50	2.11 (0.02)	19.20	1.099	
	0.05	103.6 (2.7)	17.12	60.50	
0.10	69.7 (1.1)	16.94	41.10		
0.15	51.2 (0.6)	17.17	29.80		
0.20	39.5 (1.2)	17.11	23.10		
0.30	27.0 (0.6)	17.07	15.80		
0.40	20.3 (0.5)	17.17	11.80		

^a Total ionic strength from the buffer and the contribution from [Ru(NH₃)₅py]³⁺ concentration where this is significant. ^b The standard error of the mean of multiple determinations done on one filling of the drive syringes. ^c Average second-order rate constant when two independent determinations made. ^d 25 °C, pH 5.3 acetate. ^e 25 °C, pH 5.3 acetate ($\mu = 0.25$ M), total $\mu = 0.5$ M (Na₂SO₄). ^f 25 °C, pH 6.5 phosphate.

Table III. Properties of the Reagents (25 °C)

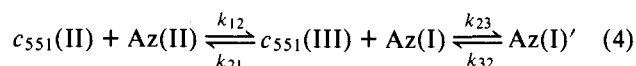
Protein	E^0 , mV, ^a vs. NHE	R , Å ^a
Ferrocyanochrome <i>c</i>	260	16.6
Stellacyanin	184	19.5
Azurin	328	17.2
HiPIP	350	15.5
Plastocyanin	350	15.8

Small molecule reagent	E^0 , mV, vs. NHE	R , Å	k_{22} , M ⁻¹ s ⁻¹
[Co(phen) ₃] ³⁺	400, ^b 370 ^c	7 ^a	4.17 × 10 ^d
[Co(bipy) ₃] ³⁺	340, ^b 315 ^e	7 ^a	1.75 × 10 ^d
[Co(terpy) ₂] ³⁺	310, ^b 270 ^{c,e}	7 ^a	2.82 × 10 ^{3f}
[Ru(NH ₃) ₅ py] ³⁺	253, ^g 273 ^e	3.5 ^h	3.38 × 10 ²ⁱ

^a Reference 11. ^b Reference 29. ^c This work, $E_{1/2}$ from cyclic voltammetry, pH 6.5 phosphate ($\mu = 0.05$ M), total $\mu = 0.1$ M (Na₂SO₄). ^d Calculated from ΔH_{22}^\ddagger and ΔS_{22}^\ddagger values obtained by H. M. Neumann (quoted in ref 29); $\mu = 0.1$ M. ^e This work, $E_{1/2}$ from cyclic voltammetry, pH 6.5 phosphate ($\mu = 0.1$ M). ^f Co(phen)₃³⁺/Co(terpy)₂²⁺, Co(bipy)₃³⁺/Co(terpy)₂²⁺, and Co(bipy)₃³⁺/Co(terpy)₃³⁺ cross-reaction rate constants at 0 °C, their activation enthalpies, and the reagent reduction potentials²⁹ were used to calculate the Co(terpy)₂^{3+/2+} k_{22} at 25 °C ($\mu = 0.1$ M), using electrostatics-corrected Marcus theory. The three k_{22} values obtained lie within a narrow range and were averaged to give 3.38 × 10² M⁻¹ s⁻¹. ^g N. Sailasuta, F. C. Anson, and H. B. Gray, unpublished results; the value of 253 mV has been obtained from spectroscopic measurements using an optically transparent thin-layer cell. The k_{22} [Ru(NH₃)₅py]^{3+/2+} calculated from this potential is 7.39 × 10² M⁻¹ s⁻¹. The calculations of ΔG_{11}^{*corr} and k_{11}^{corr} reported in Table V are based on $E = 273$ mV and $k_{22} = 3.38 \times 10^2$ M⁻¹ s⁻¹ for [Ru(NH₃)₅py]^{3+/2+}. The ΔG_{11}^{*corr} and k_{11}^{corr} parameters do not change significantly (less than 1% in most cases, and never more than 3%) if the calculations are based on $E = 253$ mV and $k_{22} = 7.39 \times 10^2$ M⁻¹ s⁻¹. ^h As the [Ru(NH₃)₅py]³⁺ ion is asymmetric, the value was averaged over individual metal–ligand radii. ⁱ This work ($\mu = 0.1$ M); calculated from the cross-reaction with Co(terpy)₂²⁺, using electrostatics-corrected Marcus theory.

the electron-transfer reaction. In this connection it should also be noted that no evidence for the formation of such a radical anion was found in the chromous reduction of pentaammineisonicotinamideruthenium(III).³⁴

It has been suggested that two forms of reduced azurin exist in equilibrium and that only one of these forms can exchange electrons with its physiological partner cytochrome *c*₅₅₁.³⁵ The mechanism proposed for electron transfer is:



where Az(I)' represents the form of azurin which cannot exchange electrons with its physiological partner. Wilson et al. have reported a value of 40 s⁻¹ (20 °C, pH 7.0, 0.1 M phos-

phate)³⁵ for k_{32} , whereas Rosen and Pecht have given a value of 11 s⁻¹ (25 °C, pH 7.0, 0.05 M phosphate).²⁴ No evidence for a redox inactive form of reduced azurin was found in our experiments with [Ru(NH₃)₅py]³⁺, but this is hardly surprising as the k_{obsd} values were always smaller than even the lower estimate of k_{32} .

Comparison of the second-order rate constants (extrapolated to $\mu = 0.1$ M, pH 6.5 phosphate) for the oxidation of the reduced proteins by [Ru(NH₃)₅py]³⁺ reveals the reactivity sequence: stellacyanin > plastocyanin > cytochrome *c* > HiPIP \approx azurin. This order matches that observed for the reduction of the proteins by [Fe(EDTA)]²⁻,¹¹ although the range of reactivity for the latter is somewhat greater, spanning 2.5 orders of magnitude compared with only two for [Ru(NH₃)₅py]³⁺. The same reactivity pattern for the blue copper(I) proteins was observed with [Co(phen)₃]³⁺,¹⁵ but, interestingly, the reactivity of ferrocyanochrome *c* toward this reagent is very much less.

The analysis described previously^{5,11} has been used to interpret the data presented here. The k_{11}^{corr} ([Ru(NH₃)₅py]³⁺) has been calculated for each protein, using the documented formulas^{5,11} and the reagent and protein properties as set out in Table III. The results are collected in Table V. Protein charges were estimated from sequence information¹¹ (and, for cytochrome *c*, extrapolated to pH values below 7.0 with the aid of titration data),³⁶ or, alternatively, were obtained from the Marcus theory fit of the ionic strength dependence for each protein–[Ru(NH₃)₅py]³⁺ redox reaction. The k_{11}^{corr} values calculated by the Marcus approach should be used for comparative purposes, as in this case a measure of internal consistency is maintained within the theoretical treatment. However, ionic strength dependence data are not available for all the inorganic reagents studied, so the k_{11}^{corr} values calculated from sequence-charge data will be used for most comparisons here.

The work term (w_{22}) is substantial for [Ru(NH₃)₅py]³⁺, owing to the small size and high charge of the reagent; this term dominates the electrostatics correction for k_{11}^{corr} . Therefore, even when the difference between the sequence and ionic strength fit charges for a protein is considerable, the k_{11}^{corr} values calculated from each will be expected to show fairly good agreement. Examination of Table V reveals that for plastocyanin(I) oxidation by [Ru(NH₃)₅py]³⁺, a difference between these two charges of four units changes k_{11}^{corr} by less than a factor of four, from 1.22 × 10⁴ to 4.76 × 10⁴ M⁻¹ s⁻¹.

In discussing the Marcus theory analysis of the data presented here, it is appropriate to draw on the interpretations and conclusions in the original treatise.¹¹ The variability in electron-transfer reactivity exhibited by protein–small molecule redox pairs is greatest when the reagent is [Fe(EDTA)]²⁻. This has been attributed to the hydrophilic nature of the reagent and the lack of extended π orbitals, which together make effective orbital overlap sensitive to small changes in protein–reagent

Table IV. Ionic Strength Dependence Fits for Oxidations by [Ru(NH₃)₅py](ClO₄)₃

Protein	Eq 1			Eq 2			Eq 3		
	Z ₁	k_0 , M ⁻¹ s ⁻¹	SE ^a	Z ₁	k_0 , M ⁻¹ s ⁻¹	SE ^a	Z ₁	k_0 , M ⁻¹ s ⁻¹	SE ^a
Ferrocyanochrome <i>c</i> ^b	11.1	2.86	4.06 (10 ²)	0.6	1.27 (10 ³)	1.06 (10 ³)	6.2	2.46 (10 ⁴)	3.80 (10 ²)
Ferrocyanochrome <i>c</i> ^c	6.5	1.81 (10 ²)	3.05 (10 ²)	0.2	5.99 (10 ³)	3.86 (10 ²)	1.8	1.34 (10 ⁴)	1.25 (10 ²)
Stellacyanin ^c	3.6	6.22 (10 ⁴)	4.14 (10 ³)	-0.2	3.33 (10 ⁵)	2.28 (10 ³)	-2.4	1.24 (10 ⁵)	9.01 (10 ³)
Azurin ^c	3.5	5.11 (10 ²)	8.51 (10)	-0.2	3.15 (10 ³)	5.34 (10)	-2.4	1.35 (10 ³)	7.7
HiPIP ^c	0.4	6.62 (10 ³)	1.15 (10 ²)	-0.4	6.09 (10 ³)	1.78 (10 ²)	-4.6	8.73 (10 ²)	3.55 (10)
Plastocyanin ^c	-0.3	1.67 (10 ⁵)	2.91 (10 ²)	-0.6	1.46 (10 ⁵)	3.12 (10 ²)	-6.1	9.17 (10 ³)	2.11 (10 ³)

^a Average error. ^b 25 °C, pH 5.3 acetate. ^c 25 °C, pH 6.5 phosphate.

Table V. Calculated Protein Self-Exchange Rate Constants (25 °C, $\mu = 0.1$ M, $w_{22} = 1.849$ kcal/mol)

Protein	Z_1^a	$k_{12}, M^{-1} s^{-1}$	$w_{12}^{b,c}$	$w_{21}^{b,c}$	$w_{11}^{b,d}$	$\Delta G_{11}^{*corr\ b}$	$k_{11}^{corr}, M^{-1} s^{-1}$
Ferrocyanochrome <i>c</i>	8.0/9.0 ^e	1.86 (10 ⁴) ^f	0.260	0.195	0.599	11.54	2.15 (10 ⁴)
	6.1/7.2 ^g	1.86 (10 ⁴) ^f	0.201	0.156	0.371	11.41	2.67 (10 ⁴)
	8.5/9.5 ^e	5.96 (10 ³) ^h	1.035	0.711	0.672	11.60	1.92 (10 ⁴)
	6.2/7.2 ^g	5.96 (10 ³) ^h	0.755	0.584	0.371	11.77	1.45 (10 ⁴)
	6.5/7.5 ⁱ	9.26 (10 ³) ^j	0.791	0.609	0.406	11.22	3.64 (10 ⁴)
	1.8/2.8 ^k	9.26 (10 ³) ^j	0.219	0.227	0.042	11.81	1.34 (10 ⁴)
Stellacyanin	0/0 ^l	1.94 (10 ⁵) ^m	0.0	0.0	0.0	10.32	1.67 (10 ⁵)
	-2.4/-1.4 ^k	1.94 (10 ⁵) ^m	-0.216	-0.084	0.016	10.64	9.70 (10 ⁴)
Azurin	-2.0/-1.0 ⁱ	2.00 (10 ³) ^m	-0.228	-0.076	0.015	12.76	2.70 (10 ³)
	-2.4/-1.4 ^k	2.00 (10 ³) ^m	-0.274	-0.106	0.025	12.85	2.34 (10 ³)
HiPIP	-3.5/-2.5 ^l	1.10 (10 ³) ⁿ	-0.130	-0.062	0.091	12.92	2.09 (10 ³)
	-4.6/-3.6 ^k	1.10 (10 ³) ⁿ	-0.172	-0.089	0.173	13.06	1.63 (10 ³)
Plastocyanin	-10.0/-9.0 ^l	7.10 (10 ³) ⁿ	-0.358	-0.215	0.882	11.87	1.22 (10 ⁴)
	-6.2/-5.1 ^k	7.10 (10 ³) ⁿ	-0.218	-0.122	0.305	11.06	4.76 (10 ⁴)

^a The two charges are for the reactant and product. ^b All energies in kilocalories/mole. ^c Work terms were calculated using the conditions of the cross-reaction. ^d Work terms were calculated for 0.1 M ionic strength. ^e The sequence data for cytochrome *c* were used to calculate the charge on the protein at pH 7.0¹¹ and titration data³⁶ were used to extrapolate to lower pH values. ^f pH 5.3 acetate ($\mu = 0.5$ M). ^g Charge obtained from Marcus theory fit of ionic strength dependence data, pH 5.3 acetate. ^h pH 5.0 acetate ($\mu = 0.1$ M). ⁱ Charge calculated from sequence data, pH 7.0.¹¹ ^j pH 6.8 phosphate ($\mu = 0.1$ M). ^k Charge from Marcus theory fit of ionic strength dependence data, pH 6.5 phosphate. ^l Charge used in ref 11, because of unreliable sequence data, for comparison purposes. ^m pH 6.5 phosphate ($\mu = 0.05$ M), total $\mu = 0.1$ M (Na₂SO₄). ⁿ pH 6.5 phosphate ($\mu = 0.25$ M), total $\mu = 0.5$ M (Na₂SO₄).

interaction and metal site accessibility. The k_{11}^{corr} values calculated from the protein-[Fe(EDTA)]²⁻ reactions have, therefore, been used to define a "kinetic accessibility" scale.

The differences in the electrostatics-corrected self-exchange activation free energies (ΔG_{11}^{*corr}) for protein redox reactions with various reagents reflect the differences in protein-reagent interaction in the transition state for electron transfer. Hence, this range in k_{11}^{corr} is also a monitor of the accessibility of the protein redox site. Although many factors may contribute to the differences in ΔG_{11}^{*corr} for a protein, probably the most important are nonelectrostatic interactions between the protein and the reagent, and breakdown of the assumption of adiabaticity (or uniform nonadiabaticity) in the original model. In some respects these two contributions are interlinked.

For example, in cytochrome *c*, nonelectrostatic interactions might be expected to permit penetration, by the reagent, of the hydrophobic residues that block the heme and, hence, facilitate electron transfer. Assuming that orbital overlap (in this case, with the heme *c*) is a measure of adiabaticity, it might also be expected that reagents with π -symmetry ligand orbitals would promote electron transfer when they are able to overlap with the porphyrin π system. Thus, the two contributions are expected to parallel one another when hydrophobic character and the availability of π -symmetry orbitals are each properties of the coordinated ligands. The activation compromise that must be reached in each redox reaction, therefore, is the attainment of maximal overlap between the heme *c* and the reagent redox orbitals at a minimal enthalpic cost for protein penetration by the reagent.

As horse heart cytochrome *c* has been the most studied electron-transfer protein to date, we will first discuss the analysis of its redox reaction data. The k_{11}^{corr} values obtained from the cross-reaction data in different media show good agreement with each other, and all of these fall into the highest of the three categories of values previously observed.¹¹ That is, the electrostatics-corrected cytochrome *c* self-exchange rate constants (k_{11}^{corr}) are ordered [Fe(EDTA)]²⁻ (6.2) \approx [Ru(NH₃)₆]²⁺ (1.6×10^4) < [Co(phen)₃]³⁺ (7.1×10^2) < [Fe(CN)₆]⁴⁻ (1.6×10^4) \approx [Ru(NH₃)₅py]³⁺ (ca. 2×10^4 M⁻¹ s⁻¹). The k_{11}^{corr} values obtained with [Fe(EDTA)]²⁻, [Ru(NH₃)₆]²⁺, and [Co(phen)₃]³⁺ have already been shown to be consistent with a mechanism of electron transfer via the partially exposed heme edge.⁵ The k_{11}^{corr} ([Ru(NH₃)₅py]³⁺) is also compatible with this mechanism, and

comparisons reveal a detailed picture of the interactions in the ferrocyanochrome *c*-[Ru(NH₃)₅py]³⁺ redox reaction.

Firstly, comparison with k_{11}^{corr} ([Ru(NH₃)₆]²⁺) shows a difference in values of three orders of magnitude, indicating that the interactions between protein and reagent in the transition state for each reaction are quite different. That is, the reagent [Ru(NH₃)₅py]³⁺ must interact with the protein surface through the pyridine moiety and not through an ammine ligand. The [Ru(NH₃)₆]²⁺ reagent, being uniformly hydrophilic, is not able to penetrate the protein surface to effect good $d\pi$ -heme edge π overlap. The hydrophobic protruding edge of the pyridine in [Ru(NH₃)₅py]³⁺, however, apparently penetrates the hydrophobic residues blocking the heme edge sufficiently to effect optimal py π -heme π overlap, thereby facilitating electron transfer.

Secondly, comparison with k_{11}^{corr} ([Co(phen)₃]³⁺) reveals a difference of 1.5 orders of magnitude in favor of reaction with [Ru(NH₃)₅py]³⁺. Good π overlap will only be realized with [Co(phen)₃]²⁺ when the porphyrin and a phenanthroline ligand are precisely aligned, and with [Ru(NH₃)₅py]³⁺ when the porphyrin is similarly aligned with the pyridine ligand. Evidently, as [Ru(NH₃)₅py]³⁺ is considerably more reactive than [Co(phen)₃]³⁺, the latter derives no benefit in this case from its extra hydrophobic character, and the controlling factor in the reaction is the size of the reagent. Thus, the enthalpic cost for [Co(phen)₃]³⁺ to penetrate in the correct orientation is too great, with the result that [Ru(NH₃)₅py]³⁺ achieves better ligand edge-heme edge π overlap (and is thus more reactive).

The ordering of the k_{11}^{corr} values for the blue copper protein plastocyanin is exactly the same as for cytochrome *c*, namely, [Fe(EDTA)]²⁻ (3.4×10^4) < [Co(phen)₃]³⁺ (2.6×10^3) < [Ru(NH₃)₅py]³⁺ (1.2×10^4 M⁻¹ s⁻¹), but the range is narrowed by an order of magnitude to ca. 2.5. The explanation for the relative reactivities is exactly analogous to that discussed for cytochrome *c*, but the fact that the range is slightly less suggests that the redox center in plastocyanin is somewhat less buried than the heme is in cytochrome *c*.

We will next discuss the results of the application of the analysis to the proteins HiPIP and azurin, as the ordering of the k_{11}^{corr} values calculated is the same. For HiPIP, [Fe(EDTA)]²⁻ (1.3×10^{-2}) < [Ru(NH₃)₆]²⁺ (2.3) < [Ru(NH₃)₅py]³⁺ (2.1×10^3) < [Co(phen)₃]³⁺ (1.4×10^4); for azurin, [Fe(EDTA)]²⁻ (1.2×10^{-2}) < [Ru(NH₃)₅py]³⁺

$(2.7 \times 10^3) < [\text{Co}(\text{phen})_3]^{3+}$ ($1.6 \times 10^4 \text{ M}^{-1} \text{ s}^{-1}$). In each case the range of reactivity is about 6 orders of magnitude, as compared to 3.5 for cytochrome *c*. This is consistent with the fact that the $\text{Fe}_4\text{S}_4\text{S}_4^*$ cluster in HiPIP is significantly more buried than the heme is in cytochrome *c*, and suggests that the redox centers in azurin and HiPIP are buried to approximately the same extent. The explanation for $[\text{Ru}(\text{NH}_3)_5\text{py}]^{3+}$ and $[\text{Ru}(\text{NH}_3)_6]^{2+}$ being more reactive with each of these proteins than $[\text{Fe}(\text{EDTA})]^{2-}$ and $[\text{Ru}(\text{NH}_3)_6]^{2+}$ is exactly the same as that given for cytochrome *c*. However, we now observe that $[\text{Co}(\text{phen})_3]^{3+}$ is more reactive toward HiPIP and azurin than is $[\text{Ru}(\text{NH}_3)_5\text{py}]^{3+}$, a reversal of their reactivity ordering toward cytochrome *c*. Inspection of space-filling molecular models reveals that the pyridine in $[\text{Ru}(\text{NH}_3)_5\text{py}]^{3+}$ can only penetrate a protein to a below-surface depth of about 4 Å before the hydrophilic surface (the amines) of the reagent will begin to interact unfavorably with hydrophobic residues. In proteins such as HiPIP, where the redox site is substantially buried (>4 Å), $[\text{Co}(\text{phen})_3]^{3+}$ is able to penetrate more extensively because of its greater overall hydrophobic character, providing that the steric constraints are not too severe. Thus, the orbital overlap of the redox centers is larger in the case of $[\text{Co}(\text{phen})_3]^{3+}$, and electron transfer from the reduced protein to Co(III) is more efficient than to the Ru(III) in $[\text{Ru}(\text{NH}_3)_5\text{py}]^{3+}$.

The last of the proteins to be discussed is the blue copper protein, stellacyanin. For this protein the k_{11}^{corr} values do not differ significantly: $[\text{Ru}(\text{NH}_3)_5\text{py}]^{3+}$ (1.7×10^5) \approx $[\text{Fe}(\text{EDTA})]^{2-}$ (2.3×10^5) \approx $[\text{Co}(\text{phen})_3]^{3+}$ ($3.0 \times 10^5 \text{ M}^{-1} \text{ s}^{-1}$). The lack of variation in k_{11}^{corr} values strongly suggests that stellacyanin employs a single mechanism of electron transfer, with a redox center that is highly kinetically accessible to each reagent. It follows that the blue copper redox center in stellacyanin must be at or within easy reach of the solvent-surface interface.

The results of the k_{11}^{corr} calculations are summarized in Figure 7, where the log of the ratio of the calculated protein self-exchange rate constant with any reagent to that with $[\text{Fe}(\text{EDTA})]^{2-}$ is plotted against $\log k_{11}^{\text{corr}}([\text{Fe}(\text{EDTA})]^{2-})$. The abscissa is a "kinetic accessibility" scale,¹¹ and the ordinate range reflects the variety of electron-transfer mechanisms employed by each protein. This range widens as the accessibility of the protein redox site decreases. The fact that $k_{11}^{\text{corr}}([\text{Ru}(\text{NH}_3)_5\text{py}]^{3+})$ is an equally good basis for an accessibility scale is shown by the remarkable linearity of $\log(k_{11}^{\text{corr}}([\text{Ru}(\text{NH}_3)_5\text{py}]^{3+})/k_{11}^{\text{corr}}([\text{Fe}(\text{EDTA})]^{2-}))$ vs. $\log k_{11}^{\text{corr}}([\text{Fe}(\text{EDTA})]^{2-})$. It is important to note, of course, that the range of protein reactivities observed with $[\text{Ru}(\text{NH}_3)_5\text{py}]^{3+}$ is narrower than that observed with $[\text{Fe}(\text{EDTA})]^{2-}$, 1.9 and 7.3 orders of magnitude, respectively. Potentially, this means that $[\text{Ru}(\text{NH}_3)_5\text{py}]^{3+}$ could be used to probe the electron-transfer reactivities of proteins that possess redox sites that are substantially more buried than the one in HiPIP.

We shall next discuss the results of the ionic strength dependence studies, and the fits of the data presented here to the theories previously described.^{5,11} However, before doing this we should reemphasize some of the major problems. All three equations (1–3) are based on a low ionic strength (Debye-Hückel) assumption, and so data would be expected to deviate from each at high ionic strengths. Equation 2 also assumes that the radii of the two reagents in the transition-state complex are equal. Clearly, this situation can never occur in protein-small molecule redox reactions and so there is no justification for applying eq 2 in such cases.

Several of the ionic strength dependences of protein-small molecule redox reactions that have been reported have been analyzed using eq 2.^{2,3,37–40} Because of fortuitous fits at low ionic strengths, protein charges have been calculated and have

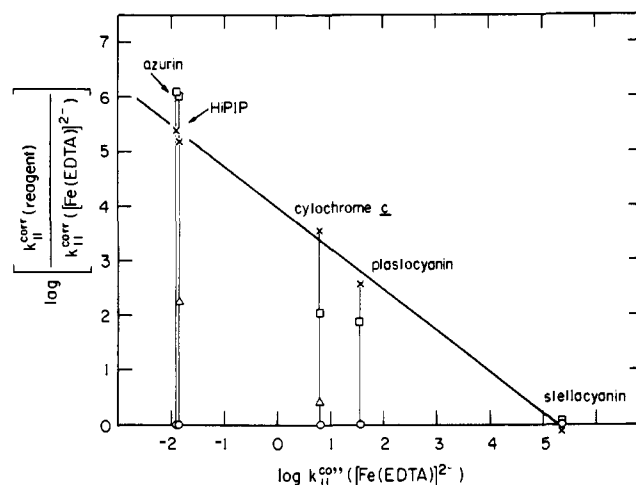


Figure 7. Plot of $\log [k_{11}^{\text{corr}}(\text{reagent})/k_{11}^{\text{corr}}([\text{Fe}(\text{EDTA})]^{2-})]$ vs. $\log k_{11}^{\text{corr}}([\text{Fe}(\text{EDTA})]^{2-})$: (□) $[\text{Co}(\text{phen})_3]^{3+}$; (×) $[\text{Ru}(\text{NH}_3)_5\text{py}]^{3+}$; (△) $[\text{Ru}(\text{NH}_3)_6]^{2+}$; (○) $[\text{Fe}(\text{EDTA})]^{2-}$.

been assigned to "active sites". These charges have then been used to define specific sites for electron transfer in the protein and, hence, have been used to differentiate among mechanistic options.³⁸ Reanalysis of these data using the Marcus theory treatment, eq 3, gives very different protein charges.¹¹ Clearly, analysis of ionic strength dependences using eq 2 is not justified, and data previously analyzed in this way are open to reinterpretation.

Examination of Table IV reveals that the Marcus theory (eq 3) gives the best fit to the ionic strength dependence data for ferrocyanochrome *c* (Figure 5), azurin(I) (Figure 6), and reduced HiPIP, whereas the transition-state theory (eq 1) yields the best fit for plastocyanin(I) (Figure 6) and stellacyanin(I). Equation 2 also gives a good fit for the latter two proteins, but, as it is not valid in these systems, we shall mainly refer to the other approaches. It is interesting that the slope of the function for the transition-state theory fit sometimes changes sign as the ionic strength increases.

The fit of the data using eq 2 consistently gives a very small protein charge ($|Z| < 1$); hence, the evolution of the "active site". The transition-state theory equation always gives a more positive value for the protein charge, which is often quite different from the sequence charge (plastocyanin, -0.3 vs. -10.0), and is sometimes even of opposite sign (azurin 3.5 vs. -2.0). The Marcus theory equation gives a charge close to that predicted from the sequence, except for stellacyanin (-2.4 vs. 10), where the sequence charge could be in serious error.¹¹

Possibly the most interesting result of these ionic strength dependence studies is the observation that ferrocyanochrome *c* behaves quite differently, in its oxidation by $[\text{Ru}(\text{NH}_3)_5\text{py}]^{3+}$, in acetate and phosphate buffers. The charge difference expected from the change in pH alone is only about 1 unit, considerably less than the difference observed, as the Marcus theory fits to the data give charges of 6.2 and 1.8 in acetate and phosphate, respectively. From these results it is clear that a specific ion effect is observed, probably attributable to the binding of phosphate ions to ferrocyanochrome *c*, thereby reducing the effective charge on the protein.

Various pieces of evidence have accumulated in favor of binding of certain ions to cytochrome *c* and which verify that this result in phosphate is reasonable. Electrophoretic mobility studies have shown that the oxidized protein binds anions, phosphate > chloride \geq iodide > sulfate > cacodylate,⁴¹ and that the reduced protein binds cations, $\text{Ca}^{2+} > \text{Mg}^{2+}$ and $\text{K}^+ \geq \text{Na}^+$.⁴² Phosphate was also postulated to bind to cytochrome *c* in certain experiments involving cytochrome oxidase.⁴³ Thermodynamic data show strong binding of anions to ferri-

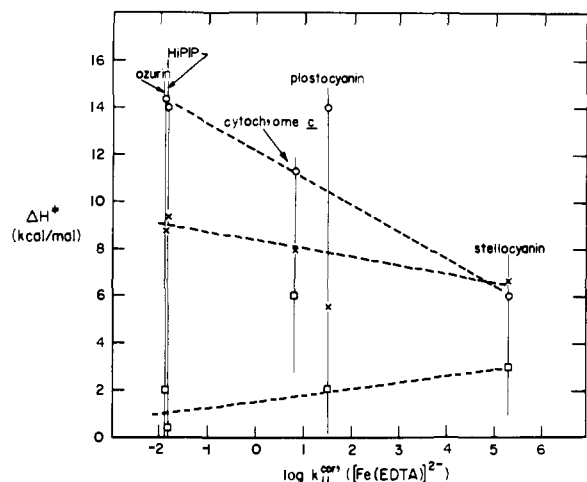


Figure 8. Plot of ΔH^\ddagger vs. $\log k_{11}^{corr}([\text{Fe}(\text{EDTA})]^{2-})$ for protein oxidations by $[\text{Ru}(\text{NH}_3)_5\text{py}]^{3+}$ (x) and $[\text{Co}(\text{phen})_3]^{3+}$ (o) and reduction by $[\text{Fe}(\text{EDTA})]^{2-}$ (o).

cytochrome *c*,⁴⁴ and cations to ferrocyanide *c*,⁴⁵ the binding constants for phosphate and chloride to the former being 4.3×10^4 and $2.0 \times 10^4 \text{ M}^{-1}$ and for Co^{2+} and Mg^{2+} to the latter of 4.9×10^3 and $7.5 \times 10^3 \text{ M}^{-1}$, respectively. These data also suggest that anions are “antibinding” to the reduced protein, and cations “antibinding” to the oxidized. However, it would be expected that ferrocyanide *c* would bind anions, at least weakly, and, in fact, under the conditions employed in the thermodynamic experiment, it would have been difficult to observe the protein-ion pairs characterized by small equilibrium binding constants. In a recent kinetic study of electron transfer between cytochrome *c* and ferro/ferricyanide, phosphate and sulfate ions were observed to compete with $[\text{Fe}(\text{CN})_6]^{3-/4-}$ for binding sites on the reduced protein, but with low affinities.⁴⁰

The suggestion that ferrocyanide *c* binds phosphate ions is qualitatively quite reasonable, but no quantitative conclusions can be made from the charge reduction of 3 to 4. Firstly, the charges calculated from the Marcus theory fits are only approximate and, therefore, the reduction in charge due to phosphate is, at best, an estimate. Secondly, the buffer contains both H_2PO_4^- and HPO_4^{2-} ions and no information is available about the relative binding abilities of each. The effective charge on the protein would also decrease with increasing ionic strength, if the binding constant were small, and although this could be accounted for in the analysis, it is hardly warranted.

As the Marcus theory fits of the data give charges close to the sequence ones, it seems reasonable that the ionic strength dependences, as observed, reflect the charge on the whole protein in the medium under investigation. It is fascinating that the ionic strength dependences that are best fit by Marcus theory involve proteins that have the more buried redox sites, on our “kinetic accessibility” scale, whereas those that are best fit by transition-state theory are associated with sites on or close to the protein surface.

Finally, we turn briefly to a consideration of the observed activation parameters. For oxidation of ferrocyanide *c* by $[\text{Ru}(\text{NH}_3)_5\text{py}]^{3+}$ at $\mu = 0.1$ and 0.5 M , these parameters are in very close agreement ($\Delta H^\ddagger = 8.0$ and 8.4 kcal/mol ; $\Delta S^\ddagger = -11$ and -14 eu , respectively) and, therefore, valid comparisons can be made among values for the various proteins, even though somewhat different experimental conditions were employed. Mechanistic arguments cannot be sustained on small changes in activation parameters (for example, $\Delta(\Delta H^\ddagger) \approx 1 \text{ kcal/mol}$; $\Delta(\Delta S^\ddagger) \approx 5 \text{ eu}$) but, nevertheless, the trends observed across the range of proteins are quite informative.

The activation parameters obtained for the reaction between $[\text{Ru}(\text{NH}_3)_5\text{py}]^{3+}$ and the outer-sphere reductant $[\text{Co}(\text{terpy})_2]^{2+}$ ($\Delta H^\ddagger = 6.2 \text{ kcal/mol}$; $\Delta S^\ddagger = -23 \text{ eu}$) most closely resemble those for the oxidation of plastocyanin. However, the parameters for each of the protein oxidation reactions lie within a very narrow energy range. The activation entropies for the oxidations of stellacyanin, ferrocyanide *c*, HiPIP, and azurin are within the range -12 to -14 eu , which is very close to the contribution expected for formation of a bimolecular collision complex from separated reactants.⁶ The activation enthalpies increase slightly across the sequence: plastocyanin < stellacyanin < ferrocyanide *c* < azurin < HiPIP, from ca. 6 to ca. 9 kcal/mol. The fact that the changes are small suggests that the mechanism in each case is an adiabatic outer-sphere one. Assuming that the activation for $[\text{Ru}(\text{NH}_3)_5\text{py}]^{3+}$ is fairly constant, that is, ΔH_{22}^\ddagger and the contribution from the reagent to ΔH_{12}^\ddagger are the same for each protein oxidation reaction, then the change in ΔH_{12}^\ddagger reflects the increasing activation of the protein. Thus, the less “kinetically accessible” the protein redox center, the greater is the enthalpic cost for protein rearrangement to give an adiabatic electron transfer process.

As shown in Figure 8, ΔH^\ddagger values also are found to increase as “kinetic accessibility” decreases for the protein oxidations by $[\text{Co}(\text{phen})_3]^{3+}$ (ca. 6 to 14 kcal/mol), although $\Delta(\Delta H^\ddagger)$ is considerably larger now. This again agrees with the k_{11}^{corr} analyses; that is, the protein activation increases considerably as the redox site becomes more buried, owing to the size of the reagent, $[\text{Co}(\text{phen})_3]^{3+}$. $[\text{Fe}(\text{EDTA})]^{2-}$, on the other hand, shows a very slight decrease in ΔH^\ddagger as the protein redox center becomes less accessible. This is consistent with a mechanism in which $[\text{Fe}(\text{EDTA})]^{2-}$ does not penetrate the protein surface at all, so that, as the redox site becomes buried, the adiabaticity of the electron-transfer reaction decreases. Thus, the major contribution to ΔH^\ddagger in these reactions is the Franck-Condon activation of the two redox centers, and there is little, if any, enthalpic cost for protein penetration.

Conclusions

By evaluating and factoring out the contributions to the activation free energy attributable to the reagent, to electrostatic (coulombic) protein-reagent interactions, and to the driving force of the overall reaction, we have shown that the electron transfer reactivity of a metalloprotein depends critically on the size and surface properties of its redox partner. From the nature of this dependence, it is apparent that electron transfer reactivity is enhanced when the substrate possesses, as does $[\text{Ru}(\text{NH}_3)_5\text{py}]^{3+}$, a hydrophobic, π -conjugated ligand that can penetrate into the interior of the protein, thereby facilitating orbital overlap with the protein redox center. Furthermore, the activation parameters for several protein-small molecule redox reactions have been shown to be generally consistent with this analysis of protein electron-transfer reactivity.

Acknowledgment. We thank Scot Wherland and Bob Scott for assistance with several calculations and for helpful discussions. This research was supported by the National Science Foundation.

Supplementary Material Available: Listing of observed pseudo-first-order rate constants (7 pages). Ordering information is given on any current masthead page.

References and Notes

- (1) Author to whom correspondence should be addressed.
- (2) H. L. Hodges, R. A. Holwerda, and H. B. Gray, *J. Am. Chem. Soc.*, **96**, 3132 (1974).
- (3) J. V. McArdle, H. B. Gray, C. Creutz, and N. Sutin, *J. Am. Chem. Soc.*, **96**, 5737 (1974).

- (4) R. X. Ewall and L. E. Bennett, *J. Am. Chem. Soc.*, **96**, 940 (1974).
 (5) S. Wherland and H. B. Gray, *Proc. Natl. Acad. Sci. U.S.A.*, **73**, 2950 (1976).
 (6) L. E. Bennett, *Prog. Inorg. Chem.*, **18**, 1 (1973).
 (7) I. A. Mizraki, F. E. Wood, and M. A. Cusanovich, *Biochemistry*, **15**, 343 (1976).
 (8) J. Rawlings, S. Wherland, and H. B. Gray, *J. Am. Chem. Soc.*, **98**, 2177 (1976).
 (9) L. E. Bennett, "The Iron-Sulfur Proteins". Vol. III. W. Lovenberg, Ed., Academic Press, New York, N.Y., 1976, Chapter 9.
 (10) C. W. Carter, Jr., J. Kraut, S. T. Frear, and R. A. Alden, *J. Biol. Chem.*, **249**, 6339 (1974).
 (11) S. Wherland and H. B. Gray, In "Biological Aspects of Inorganic Chemistry", D. Dolphin, Ed., Wiley, New York, N.Y., 1977, p 289.
 (12) E. I. Solomon, J. W. Hare, and H. B. Gray, *Proc. Natl. Acad. Sci. U.S.A.*, **73**, 1389 (1976).
 (13) S. Wherland, R. A. Holwerda, R. C. Rosenberg, and H. B. Gray, *J. Am. Chem. Soc.*, **97**, 5260 (1975).
 (14) R. C. Rosenberg, S. Wherland, R. A. Holwerda, and H. B. Gray, *J. Am. Chem. Soc.*, **98**, 6364 (1976).
 (15) J. V. McArdle, C. L. Coyle, H. B. Gray, G. S. Yoneda, and R. A. Holwerda, *J. Am. Chem. Soc.*, **99**, 2483 (1977).
 (16) R. P. Ambler and M. Wynn, *Biochem. J.*, **131**, 485 (1973).
 (17) P. Ford, De F. P. Rudd, R. Gaunder, and H. Taube, *J. Am. Chem. Soc.*, **90**, 1187 (1968).
 (18) It was found that scaling up this preparation resulted in a much lower percent yield of product: thus, several batches of $[\text{Ru}(\text{NH}_3)_5\text{py}](\text{ClO}_4)_2$ were prepared as described, and were pooled for conversion to the ruthenium(III) species.
 (19) In general, elemental analyses of ruthenium perchlorates were found to be inconsistent. The purity of the compound was checked by differential pulsed polarography, and by reproducibility ($\pm 1\%$) of the oxidation kinetics with ferrocycochrome c.
 (20) B. R. Baker, F. Basolo, and H. M. Neumann, *J. Phys. Chem.*, **83**, 371 (1959).
 (21) $[\text{Ru}(\text{NH}_3)_5\text{py}]^{3+}$ was found to be unstable under the following conditions: (1) in any medium above pH 7.0; (2) at any pH in the presence of chloride; (3) in any medium containing a "good" ligand for Ru^{III} . The mechanism of decomposition, in any of these cases, could involve disproportionation of $\text{Ru}(\text{III})$, substitution, or catalyzed reduction of $\text{Ru}(\text{III})$ or any complex combination, but no detailed study of this was carried out.
 (22) E. Margolias and N. Frohwirt, *Biochem. J.*, **71**, 570 (1969).
 (23) B. G. Malmström, B. Reinhammar, and T. Vänngård, *Biochim. Biophys. Acta*, **205**, 48 (1970).
 (24) P. Rosen and I. Pecht, *Biochemistry*, **15**, 775 (1976).
 (25) P. R. Milne and J. R. E. Wells, *J. Biol. Chem.*, **245**, 1566 (1970).
 (26) R. G. Bartsch, "Bacterial Photosynthesis", H. Gest, A. San Pietro, and L. Vernon, Ed., Antioch Press, Yellow Springs, Ohio, 1963, p 315.
 (27) For any reaction of the type $A + B \rightleftharpoons C + D$, which is pseudo first order in B in the forward direction and second order in reverse, the integrated rate equation is:

$$\ln \left[\frac{A_0^2 - A_e A_t}{A_0(A_t - A_e)} \right] = \left[\frac{A_0 + A_e}{A_0 - A_e} \right] kt$$

where A_0 = concentration of A at time = 0, A_t = concentration of A at time t , and A_e = concentration of A at equilibrium. In the oxidation of azurin(I) by $[\text{Ru}(\text{NH}_3)_5\text{py}]^{3+}$, as azurin(II) is the only absorbing species, the equation can be simplified to give:

$$\ln [Abs_\infty(Abs_t + Abs_e) - Abs_t Abs_e] - \ln [Abs_\infty(Abs_e - Abs_t)] = \left[\frac{2Abs_\infty - Abs_e}{Abs_e} \right] kt$$

where Abs_∞ = absorbance for reaction completion ($>99\%$), Abs_e = absorbance at equilibrium, and Abs_t = absorbance at time t , and so the rate constant (k) can be computed easily from absorbance vs. time data.

- (28) Data were generated for a hypothetical reaction approaching equilibrium, where the forward reaction went to 75% completion (actual absorbance change = $0.75 \times$ expected absorbance change). These data were then fitted to both the equilibrium equation and the simple first-order decay:

$$\log \frac{(A_0 - A_\infty)}{(A_t - A_\infty)} = kt$$

The rate constant obtained from the linear portion of the slope of the latter was ca. 50% higher than that used in the equilibrium equation to generate the data. The importance of these observations is that a reaction which is proceeding to equilibrium rather than to completion may appear linear in a simple first-order plot for 70–80% of the absorbance change, especially if this is small, and only show slight curvature over 3 half-lives. The data *should not* be refitted by the Guggenheim method, as there is *no* justification for a reanalysis involving a different absorbance baseline. For reactions to reach $\geq 90\%$ completion, k_{obsd} will be less than 10% in error of the true rate constant, but for any other equilibrium situation the full analysis should be employed. Criteria, external to the actual data collection, should be used to recognize the equilibrium situation and prevent misinterpretation of data.

- (29) R. Farina and R. G. Wilkins, *Inorg. Chem.*, **7**, 514 (1968).
 (30) Studies on the nature of the products of the preparation of $[\text{Co}(\text{phen})_3]^{3+}$ and $[\text{Co}(\text{bipy})_3]^{3+}$ and related species under various conditions,³¹ and on the decomposition of $[\text{Co}(\text{phen})_3]^{3+}$ in the presence of halide ions and light,³² suggest that $[\text{Co}(\text{phen})_3]^{3+}$, and probably $[\text{Co}(\text{bipy})_3]^{3+}$ and $[\text{Co}(\text{terpy})_2]^{3+}$, are susceptible to some decomposition under the conditions employed for the cyclic voltammograms. $[\text{Ru}(\text{NH}_3)_5\text{py}]^{3+}$ has also been observed to decompose in these media. Thus, the extraneous peaks in the anodic and cathodic half-cycles are probably attributable to species formed in reactions with the medium.
 (31) (a) J. G. Gibson, R. Laird, and E. D. McKenzie, *J. Chem. Soc. A*, 2089 (1969); (b) J. G. Gibson and E. D. McKenzie, *ibid.*, 2478 (1970).
 (32) R. J. Mureinik, *Inorg. Nucl. Chem. Lett.*, **12**, 319 (1976).
 (33) D. Cummins and H. B. Gray, unpublished results.
 (34) R. G. Gaunder and H. Taube, *Inorg. Chem.*, **9**, 2627 (1970).
 (35) M. T. Wilson, C. Greenwood, M. Brunori, and E. Antonini, *Biochem. J.*, **145**, 449 (1975).
 (36) (a) H. B. Bull and K. Breese, *Biochem. Biophys. Res. Commun.*, **24**, 1 (1966); (b) R. W. Shaw and C. R. Hartzell, *Biochemistry*, **15**, 1909 (1976).
 (37) F. E. Wood and M. A. Cusanovich, *Bioinorg. Chem.*, **4**, 337 (1975).
 (38) (a) F. E. Wood and M. A. Cusanovich, *Arch. Biochem. Biophys.*, **168**, 333 (1975); (b) M. A. Cusanovich, *Bioorg. Chem.*, in press.
 (39) W. G. Miller and M. A. Cusanovich, *Biophys. Struct. Mech.*, **1**, 97 (1975).
 (40) Y. Ilan, A. Shafferman, and G. Stein, *J. Biol. Chem.*, **251**, 4336 (1976).
 (41) G. Barlow and E. Margolias, *J. Biol. Chem.*, **241**, 1473 (1966).
 (42) E. Margolias, G. H. Barlow, and V. Byers, *Nature (London)*, **228**, 723 (1970).
 (43) S. Ferguson-Miller, D. L. Brautigan, and E. Margolias, *J. Biol. Chem.*, **251**, 1104 (1976).
 (44) R. Margalit and A. Schejter, *Eur. J. Biochem.*, **32**, 500 (1973).
 (45) R. Margalit and A. Schejter, *Eur. J. Biochem.*, **46**, 387 (1974).